An EKF formulation for pose estimation of a landing platform fixed to a moving vehicle for an autonomous landing system

Eder A. Moura[1], Luiz C. S. Góes[1]

[1]*Departamento de Mecatrônica, Instituto Tecnológico de Aeronáutica*
Praça Marechal Eduardo Gomes, nº 50, 12228-900, SP/São José dos Campos, Brasil
edermoura@ufu.br, goes@ita.br

Abstract. Automatic landing systems are heavily dependent on sensors to map the environment around the aircraft in order to support the subsequent control strategy to accomplish the task. This work proposes a discrete-time Extended Kalman Filter (EKF) formulation, using camera measurements, to estimate the position and orientation (yaw) states of a landing platform, fixed on top of a Ground Vehicle (GV). GV moves freely at constant speed The camera is attached to an Unmanned Aerial Vehicle (UAV) and is pointed down. For each image taken by the camera, a computer vision algorithm returns the relative position and attitude (pose) of each identified marker. Its is adopted the open-source library Aruco for generating the printable square-based fiducial markers. Its adoption is justified because it allows quick fixation to the landing platform, being easily detectable and providing a robust determination of the relative pose. The EKF is formulated as a constant velocity model for the pose estimation. The simulation consists of the UAV following the GV along a path, where the desired states are estimated from noise-corrupted measurements. The proposition is validated via Monte Carlo simulation. The results showed that the proposed formulation for the EKF is able to estimate the desired states when operating at low speeds.

Keywords: pose estimation, uav, ground vehicle, automatic landing, aruco.

1 Introduction

Cooperation between Ground Vehicles (GV) and Unmanned Aerial Vehicles (UAVs) allows the development of many applications that exploit the advantages of each vehicle. This combination helps to circumvent the limitations of each vehicle, as the energy storage capacity of the batteries for small UAVs and the surrounding exploration and mapping for GVs. In this scenario, the use of autonomous vehicles expands the possibilities of applying these technologies in cooperative activities. Considering that both vehicles are moving, the autonomous landing system embedded in the UAV needs to estimate the states that describes the GV movement. To this end, this work proposes an estimation system based on the Extended Kalman Filter (EKF) formulation, using camera measurements to estimate the position and orientation (yaw) of a landing platform (LP) fixed on top of the GV. The proposed solution explores the properties of quaternion algebra in the EKF formulation and the use of artificial planar markers as strategy to easily embed the algorithm in flight controllers of small UAVs. The formulation is validated by a Monte Carlo simulation.

The rest of this paper is organized as follows: Section 2 begins by presenting some necessary concepts required in the developments, the geometrical relations in the formulation and presents the dynamic model for the GV and UAV; Section 3 present the EKF algorithm and states the equations proposed to solve the estimation problem; Section 4 details the simulation process and shows the results obtained; and, finally, a conclusion is presented in Section 5.

2 Problem definition and system modeling

The estimation system proposed in this work is to be used in an automatic landing system for a UAV (a quadrotor) to land in a platform fixed on top of a GV (a car). A representation of this scenario is shown in Fig.

1a. For this operation, the UAV is equipped with sensors to estimate its position and attitude with respect to an external reference frame. The GV moves at a constant speed and travels an unpredictable path. There will be no data exchange between the GV and the UAV.

To ease the estimation of LP pose states, five ARUCO markers were printed and fixed on it, as can be seen in Fig. 1c. The Aruco markers are artificial square-based fiducial markers, proposed in Garrido-Jurado et al. [1] and Romero-Ramirez et al. [2], that allows to obtain the relative three dimensional position and attitude of each marker with respect to the camera. Thus, the objective is to estimate the LP states through these indirect measures.

2.1 Fundamental concepts and definitions

Before beginning the description of the system's model, this section presents a set of conventions that will be adopted throughout the text.

Scalars are represented by lowercase letters as $a \in \mathbb{R}$, algebraic vectors are column matrices represented by bold lowercase letters as $\mathbf{a} \in \mathbb{R}^n$ and matrices are represented by bold uppercase letters $\mathbf{A} \in \mathbb{R}^{p\times q}$. The transpose vectors and matrices are respectively indicated by $\mathbf{a}^\top$ and $\mathbf{A}^\top$. The inverse matrix is denoted as $\mathbf{A}^{-1}$. Also, $\mathbf{I}_n \in \mathbb{R}^{n\times n}$ is an identity matrix, with ones in the main diagonal and zeros elsewhere. The algebraic projection of geometric vector $\vec{a}$ in a Cartesian coordinate systems (CCS) $\mathcal{S}_A$ is denoted as $\mathbf{a}_A$. The direction cosine matrix (DCM) $\mathbf{D}^{B/A} \in SO(3)$ represents the attitude of $\mathcal{S}_B$ w.r.t. $\mathcal{S}_A$. $SO(3)$ is a matrix of the *special orthogonal group of order 3* and implies that $\mathbf{D}^{A/B} = \left(\mathbf{D}^{B/A}\right)^\top = \left(\mathbf{D}^{B/A}\right)^{-1}$ and its determinant is equal to 1. It is such that the representation of a vector $\vec{a}$ in $\mathcal{S}_B$ and $\mathcal{S}_A$ is related by $\mathbf{a}_B = \mathbf{D}^{B/A}\mathbf{a}_A$ and the transformation in the opposite direction is denoted by $\mathbf{a}_A = \left(\mathbf{D}^{B/A}\right)^{-1}\mathbf{a}_B$. This work often parameterizes the DCM by a quaternion of rotation that is a four-component vector with some operations defined on it. Its general form is represented as $\mathbf{q} \triangleq \left[\mathbf{q}_{1:3}^\top \; q_4\right]^\top \in \mathbb{R}^4$, where $\mathbf{q}_{1:3} \triangleq \left[q_1 \; q_2 \; q_3\right]^\top \in \mathbb{R}^3$. An explanation of attitude representation by quaternions and its properties can be found in Shuster [3] and Markley and Crassidis [4].This work adopts the notation presented in the last one. Two important operations are the quaternion products $\mathbf{q}^A \otimes \mathbf{q}^B$ and $\mathbf{q}^A \odot \mathbf{q}^B$, as stated in Pittelkau [5]. For the pair of quaternions $\mathbf{q}^A$ and $\mathbf{q}^B$, these products can be expressed as matrix products, defined by:

$$\mathbf{q}^A \otimes \mathbf{q}^B = \left[\mathbf{q}^A \otimes\right]\mathbf{q}^B = \begin{bmatrix} q_4^A\mathbf{I}_3 - \left[\mathbf{q}_{1:3}^A \times\right] & \mathbf{q}_{1:3}^A \\ -\left(\mathbf{q}_{1:3}^A\right)^\top & q_4^A \end{bmatrix}\mathbf{q}^B, \text{ and} \tag{1}$$

$$\mathbf{q}^A \odot \mathbf{q}^B = \left[\mathbf{q}^A \odot\right]\mathbf{q}^B = \begin{bmatrix} q_4^A\mathbf{I}_3 + \left[\mathbf{q}_{1:3}^A \times\right] & \mathbf{q}_{1:3}^A \\ -\left(\mathbf{q}_{1:3}^A\right)^\top & q_4^A \end{bmatrix}\mathbf{q}^B, \text{ where} \tag{2}$$

$$\left[\mathbf{q}_{1:3} \times\right] \triangleq \begin{bmatrix} 1 & -q_3 & q_2 \\ q_3 & 1 & -q_1 \\ -q_2 & q_1 & 1 \end{bmatrix} \in \mathbb{R}^{3\times 3} \tag{3}$$

is the skew-symmetric matrix of the vector $\mathbf{q}_{1:3}$. Note that $\mathbf{q}^A \otimes \mathbf{q}^B = \mathbf{q}^B \odot \mathbf{q}^A$.

The DCM parameterization by $\mathbf{q}$ is defined as: $\mathbf{D}^{B/A}\left(\mathbf{q}^{B/A}\right) \triangleq \left(q_4^2 - \|\mathbf{q}\|^2\right)\mathbf{I}_3 - 2q_4\left[\mathbf{q}_{1:3} \times\right] + 2\mathbf{q}_{1:3}\mathbf{q}_{1:3}^\top$ and requires that $\|\mathbf{q}\| = 1$. Note that $\mathbf{D}^{D/A}\left(\mathbf{q}^{D/A}\right) = \mathbf{D}^{D/C}\left(\mathbf{q}^{D/C}\right)\mathbf{D}^{C/B}\left(\mathbf{q}^{C/B}\right)\mathbf{D}^{B/A}\left(\mathbf{q}^{B/A}\right)$ represents successive rotations, that is equivalent to the quaternion operations $\mathbf{q}^{D/A} = \mathbf{q}^{D/C} \otimes \mathbf{q}^{C/B} \otimes \mathbf{q}^{B/A}$, and $\left(\mathbf{D}^{B/A}\right)^{-1} \equiv \left[\left(\mathbf{q}^{B/A}\right)^{-1} \otimes\right]$. Thus, considering the schematic view present in Fig. 1b, the position vector $\vec{p}^{\,i}$ and the attitude $\mathbf{q}^{i/R}$ w.r.t. $\mathcal{S}_R$, for $i = 1, \ldots, 5$, are related to the measurements taken by the camera at the UAV by:

$$\vec{p}^{\,i} = \vec{r} + \vec{c} + \vec{s}^{\,i}, \text{ and} \tag{4}$$

$$\mathbf{q}^{i/R} = \mathbf{q}^{i/C} \otimes \left(\mathbf{q}^{B/C}\right)^{-1} \otimes \mathbf{q}^{B/R}, \tag{5}$$

where $\vec{r}$ is the position vector of $\mathcal{S}_B$ (UAV position) with respect to (w.r.t.) $\mathcal{S}_R$; $\vec{c}$ is the position vector of $\mathcal{S}_C$ (camera position) w.r.t. $\mathcal{S}_B$ - that is $\vec{0}$ for this case; $\vec{s}^{\,i}$ is position of the center of each marker $\mathcal{S}_P^i$ w.r.t. $\mathcal{S}_C$ –

each marker has an unique identifier number, made available when the marker is detected in the processing of each frame; and $\mathcal{S}_P$ is the the LP CSS that is coincident with $\mathcal{S}_P^1$, as shown in Fig. 1c.

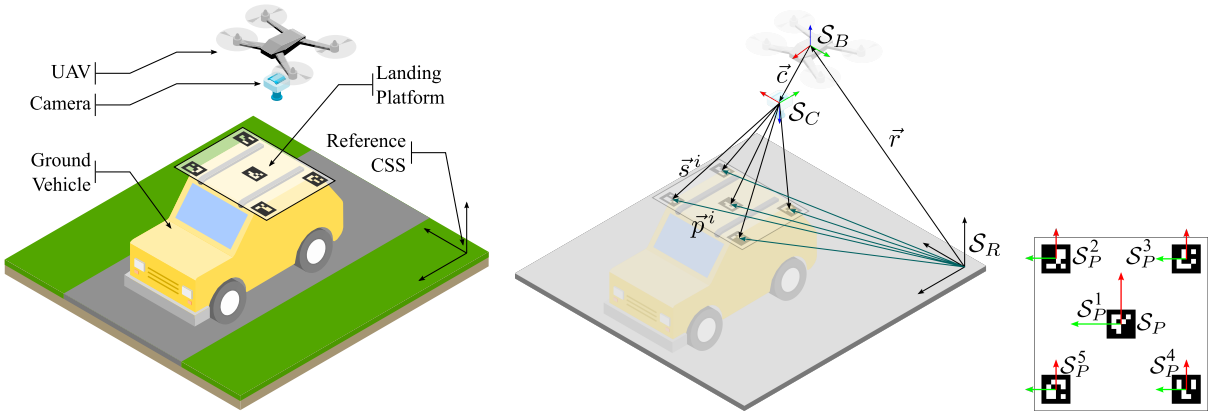

(a) Description of the components involved in the modeling.

(b) Diagram of the geometric relationship of the CCSs adopted in the modeling.

(c) Landing platform with five ARUCO markers.

Figure 1. Representation of model components and visualization of their geometric relationships. The red, green, and blue colors of the coordinate systems represent the x-axis, y-axis, and z-axis, respectively.

2.2 Ground Vehicle Model

The GV is usually modeled by the so-called bicycle model, as described by Popp and Schiehlen [6] and Polack et al. [7]. An adapted version is adopted here and the planar movement of the GV is modeled by the following set of non-linear equations:

$$\begin{bmatrix} \dot{x}^g \\ \dot{y}^g \\ \dot{\alpha} \\ \dot{\theta} \end{bmatrix} = \begin{bmatrix} v\cos(\alpha) \\ v\sin(\alpha) \\ v\frac{\tan(\theta)}{d} \\ \frac{-1}{\tau_s}\theta + \frac{1}{\tau_s}\bar{\theta} \end{bmatrix}, \tag{6}$$

where: $\mathbf{g} \triangleq [x^g\ y^g\ \alpha\ \theta]^\top$ is the state vector of the GV model; x^g and y^g are the GV position in $\mathcal{S}_R$; α is the orientation angle, formed by the longitudinal axis of the GV w.r.t the x-axis of $\mathcal{S}_R$; $\theta \in [-\theta_{max}, \theta_{max}]$ is the steering angle of the wheels in relation to the longitudinal axis of the GV; v is the modulus of the linear velocity of the vehicle; d is the wheelbase of the GV; and τ_s is the time constant of the steering wheel control.

2.3 Unmanned Aerial Vehicle Model

A UAV dynamics is modeled by the set of nonlinear equations, as developed by Mahony et al. [8], and this work adopts the following model:

$$\begin{bmatrix} \dot{\mathbf{w}} \\ \dot{\mathbf{r}}_R \\ \dot{\mathbf{v}}_R \\ \dot{\mathbf{q}}^{B/R} \\ \dot{\boldsymbol{\omega}}_R \end{bmatrix} = \begin{bmatrix} \frac{1}{\tau_m}\left(-\mathbf{w} + k_m\bar{\mathbf{w}}\right) \\ \mathbf{v}_R \\ \frac{1}{m}\left[0\ 0\ F^C\right]^\top + \frac{1}{m}\mathbf{F}^g \\ \frac{1}{2}\boldsymbol{\Xi}\left(\mathbf{q}^{B/R}\right)\boldsymbol{\omega}_R \\ \mathbf{J}^{-1}\Big[\left(\mathbf{J}\boldsymbol{\omega}_R\right)\times\Big]\boldsymbol{\omega}_R + \mathbf{J}^{-1}\mathbf{T}_R^C \end{bmatrix}, \tag{7}$$

where the settling time τ_m and the proportional gain k_m are constants for the motor and propeller assembly, that can be obtained experimentally; $\mathbf{w} \triangleq [w_1\ w_2\ w_3\ w_4]^\top \in \mathbb{R}^4$ are the current rotation speed of the propellers, with

$w_j \in [0, w_{max}]$, for $j = 1, \ldots, 4$; $\bar{\mathbf{w}} \triangleq [\bar{w}_1\ \bar{w}_2\ \bar{w}_3\ \bar{w}_4]^\top \in \mathbb{R}^4$ are the commands of rotational speed for the propellers; and $\mathbf{r}_R \triangleq [r_1\ r_2\ r_3]^\top \in \mathbb{R}^3$ and $\mathbf{v}_R \triangleq [v_1\ v_2\ v_3]^\top \in \mathbb{R}^3$ are the linear position and velocity of $\mathcal{S}_B$ w.r.t $\mathcal{S}_R$; $\mathbf{q}^{B/R}$ and $\boldsymbol{\omega} \triangleq [\omega_1\ \omega_2\ \omega_3]^\top \in \mathbb{R}^3$ are the attitude and angular velocity of $\mathcal{S}_B$ w.r.t $\mathcal{S}_R$. The constants $m \in \mathbb{R}$ and $J \in \mathbb{R}^{3\times3}$ are, respectively, the mass and the rotational inertia matrix (a diagonal matrix expressed as $diag(J_x, J_y, J_z)$). The rotation of the propellers results in thrust forces $\mathbf{f} \triangleq [f_1\ f_2\ f_3\ f_4]^\top \in \mathbb{R}^4$ and, due the drag effect, a reaction torque $\mathbf{d} \triangleq [d_1\ d_2\ d_3\ d_4]^\top \in \mathbb{R}^4$, where $f_i = k_t w_i^2$ and $d_i = (-1)^{i+1} k_d w_i^2$, for $i = 1, 2, 3, 4$, with k_t and k_d being constants experimentally determined. Thus, the modulus of the thrust force $F^C \in \mathbb{R}$ along the z-axis of $\mathcal{S}_\text{B}$ and the control torque $\mathbf{T}_R^C \in \mathbb{R}^3$ are obtained by the following relation:

$$\begin{bmatrix} F^C \\ \mathbf{T}_R^C \end{bmatrix} = \begin{bmatrix} 1 & 1 & 1 & 1 \\ l_1 & -l_1 & -l_1 & l_1 \\ -l_2 & -l_2 & l_2 & l_2 \\ k_{dt} & -k_{dt} & k_{dt} & -k_{dt} \end{bmatrix} \mathbf{f}, \tag{8}$$

where l_1 is the distance from the front and back rotors to $\mathcal{S}_B$'s y-axis; l_2 is the lateral distance of the rotors to $\mathcal{S}_B$'s x-axis; and $k_{dt} = \frac{k_d}{k_t}$.

3 Filter formulation

As described in Fang et al. [9] and Bar-Shalom et al. [10], the EKF is a sub-optimal solution to the problem of state estimation in the minimum mean-squared error (MMSE) sense, by linearize the nonlinear system dynamic and measurement models about the current estimated state, using the first-order Taylor series approximation. Assuming that the nonlinear system can be described by the set of discrete-time difference equations:

$$\mathbf{x}_{k+1} = \mathbf{f}_k\left(\mathbf{x}_k, \mathbf{u}_k\right) + \mathbf{w}_k, \text{ and} \tag{9}$$

$$\mathbf{y}_{k+1} = \mathbf{h}_{k+1}\left(\mathbf{x}_{k+1}\right) + \mathbf{v}_{k+1}, \tag{10}$$

where the eq. (9) is the system dynamics and the eq. (10) the measurement model, $\mathbf{x}$ is the state vector; $\mathbf{u}$ is a known input; $\mathbf{f}_k(\cdot)$ and/or $\mathbf{h}_k(\cdot)$ have some nonlinear term, with $\mathbf{w}_k$ and $\mathbf{v}_{k+1}$ representing, respectively, the process noise and the measurement noise, which are modeled as uncorrelated, zero mean, white Gaussian processes, whose covariances are defined by the matrices $\mathbf{Q}_k$ and $\mathbf{R}_k$; the initial conditions being $\hat{\mathbf{x}}_0 = \mathbf{x}(0) \in \mathbb{R}^n$ and $\mathbf{P}_0 = \mathbf{P}(0) \in \mathbb{R}^{n\times n}$, for $k \in \mathbb{Z}^*$; the EKF algorithm is stated as the two steps (prediction and update) given by:

Prediction:

$$\begin{aligned} \hat{\mathbf{x}}_{k+1}^- &= \mathbf{f}_k(\hat{\mathbf{x}}_k, \mathbf{u}_k) \\ \mathbf{P}_{k+1}^- &= \mathbf{F}_k \mathbf{P}_k \mathbf{F}_k^\top + \mathbf{Q}_k \end{aligned}$$

Update:

$$\begin{aligned} \hat{\mathbf{y}}_{k+1} &= \mathbf{h}_{k+1}(\hat{\mathbf{x}}_{k+1}^-) \\ \mathbf{P}^Y &= \mathbf{H}_{k+1} \mathbf{P}_{k+1}^- \mathbf{H}_{k+1}^\top + \mathbf{R}_{k+1} \\ \mathbf{P}^{XY} &= \mathbf{P}_{k+1}^- \mathbf{H}_{k+1}^\top \\ \mathbf{K} &= \mathbf{P}^{XY} \left(\mathbf{P}^Y\right)^{-1} \\ \hat{\mathbf{x}}_{k+1}^+ &= \hat{\mathbf{x}}_{k+1}^- + \mathbf{K}\left(\mathbf{y}_{k+1} - \hat{\mathbf{y}}_{k+1}\right) \\ \mathbf{P}_{k+1}^+ &= \left(\mathbf{I} - \mathbf{K}\mathbf{H}_{k+1}\right) \mathbf{P}_{k+1}^- \left(\mathbf{I} - \mathbf{K}\mathbf{H}_{k+1}\right)^\top + \mathbf{K}\mathbf{R}_{k+1}\mathbf{K}^\top \end{aligned}$$

where $\hat{\mathbf{x}} \in \mathbb{R}^n$ is estimated state vector; $\mathbf{P} \in \mathbb{R}^{n\times n}$ is the covariance matrix of $\hat{\mathbf{x}}$; $\mathbf{y}_{k+1} \in \mathbb{R}^m$ is the measurement vector; $\mathbf{F} = \frac{\partial \mathbf{f}_k(\cdot)}{\partial \hat{\mathbf{x}}} \in \mathbb{R}^{n\times n}$; and $\mathbf{H} = \frac{\partial \mathbf{h}_k(\cdot)}{\partial \hat{\mathbf{x}}} \mathbb{R}^{m\times n}$.

Adopting a discrete-time model of constant linear velocity and constant angular velocity (parameterized by a quaternion), the state equation of the EKF is:

$$\begin{bmatrix} \mathbf{p}^i_{Rk+1} \\ \mathbf{v}^i_{Rk+1} \\ \vdots \\ \mathbf{q}^{P/R}_{k+1} \\ \boldsymbol{\omega}_{k+1} \end{bmatrix} = \begin{bmatrix} \begin{bmatrix} \mathbf{I}_3 & T_s\mathbf{I}_3 \\ \mathbf{0}_{3\times3} & \mathbf{I}_3 \end{bmatrix} \begin{bmatrix} \mathbf{p}^i_{Rk} \\ \mathbf{v}^i_{Rk} \end{bmatrix} \\ \vdots \\ \mathbf{q}^{P/R}_k + \frac{T_s}{2}\boldsymbol{\Xi}\left(\mathbf{q}^{P/R}_k\right)\boldsymbol{\omega}_k \\ \boldsymbol{\omega}_k \end{bmatrix}, \tag{11}$$

where the state vector is defined by $\mathbf{x} \triangleq \left[(\mathbf{p}^1_R)^\top \ (\mathbf{v}^1_R)^\top \ \dots \ (\mathbf{p}^5_R)^\top \ (\mathbf{v}^5_R)^\top \ (\mathbf{q}^{P/R})^\top \ (\boldsymbol{\omega})^\top\right]^\top \in \mathbb{R}^{37}$; $\mathbf{p}^i$ and $\mathbf{v}^i$ correspond, respectively, to the linear position and velocity of the i-th maker; and $\mathbf{q}$ and $\boldsymbol{\omega}$ are, respectively, the parameterized yaw angle and the angular velocity of the LP; $T_s[s]$ is the step time between the samples; $i = 1, \dots, 5$; and $\boldsymbol{\Xi}(\mathbf{q}) \triangleq \begin{bmatrix} q_4\mathbf{I}_3 + [\mathbf{q}_{1:3}\times] \\ -\mathbf{q}^\top_{1:3} \end{bmatrix}$.

The measurement equation obtains five relative position vectors of the planar artificial markers w.r.t. $\mathcal{S}_C$ and also five relative attitude vectors $\mathbf{q}^{i/C} \equiv \mathbf{q}^{P/C}$, for $i = 1, \dots, 5$, which are ideally equals, since all markers are aligned in the LP, as shown in Fig. 1c. Thus, the measurement model is defined by:

$$\begin{bmatrix} \mathbf{p}^1_{Rk+1} \\ \vdots \\ \mathbf{p}^5_{Rk+1} \\ \mathbf{q}^{1/C}_{k+1} \\ \vdots \\ \mathbf{q}^{5/C}_{k+1} \end{bmatrix} = \begin{bmatrix} \left(\mathbf{D}^{B/C}\right)^\top \mathbf{D}^{B/R}(\mathbf{q}^{B/R})\left(\mathbf{p}^1_R - \mathbf{r}_R\right) \\ \vdots \\ \left(\mathbf{D}^{B/C}\right)^\top \mathbf{D}^{B/R}(\mathbf{q}^{B/R})\left(\mathbf{p}^5_R - \mathbf{r}_R\right) \\ \mathbf{q}^{B/C} \odot \left(\mathbf{q}^{B/R}\right)^{-1} \odot \mathbf{q}^{P/R} \\ \vdots \\ \mathbf{q}^{B/C} \odot \left(\mathbf{q}^{B/R}\right)^{-1} \odot \mathbf{q}^{P/R} \end{bmatrix}. \tag{12}$$

4 Simulation and Results

An overview of the estimation system and its relationship to the entire system is presented in Fig. 2. For this proposal, a sampling time of $T_s = 35\ [ms]$ was adopted for the EKF, considering $25\ [ms]$ to acquire the frame plus $10\ [ms]$ of processing time. The estimation was evaluated for three cases of GV speed: C1) $v = 3\ [m/s]$; C2) $v = 6\ [m/s]$; and C3) $v = 12\ [m/s]$. The evaluation of the statistical properties of the estimated states was conduced by Monte Carlo method, a numerical inference based on sampling of simulated (pseudo-)random data, with 100 runs per case. For each run, a random zero-mean Gaussian noise is added to the measurements, with standard deviation of $\pm 0.1\ [m]$ for $\mathbf{s}^{i/C}$ and $\pm 5^\circ$ for $\mathbf{q}^{i/C}$. For each of the three cases analyzed, the final estimated value for the path $\hat{p}_k \triangleq [x_k\ y_k]^\top$ and orientation $\hat{\alpha}_k$ for each marker is computed by the average of the ensemble of 100 executions, at each sample time. The estimation error ϵ is computed by an Euclidean norm, between the true value and the mean of the ensemble.

The GV and UAV are simulated with eq. (6) and eq. (7), respectively, using a 4$^{\text{th}}$-order Runge-Kutta method, with a constant step time of $h = 1\ [ms]$. Table 1 contain the parameters of the vehicles adopted in the simulation. The UAV starts at $\mathbf{r}_0 = [0\ 0\ 10]^\top\ [m]$ and the GV at $[x^g_0\ y^g_0]^\top = [0\ 0]^\top\ [m]$. The UAV follows the GV position along the path. The LP is assumed to be at $1.6\ [m]$ above the ground and the UAV descends to $0.4\ [m]$ above the LP. The GV is commanded to follows the path generated by:

$$\bar{y}^g(x^g) = 30\sin\left(2\pi\frac{1}{500}x^g\right) + 20\sin\left(2\pi\frac{1}{200}x^g\right)[m]. \tag{13}$$

The results of the simulations are summarized in the Fig. 3, Fig. 4, and Fig. 5. In all these cases, the ability to estimate the position and orientation states of the LP by the proposed formulation are demonstrated. However, the estimation error increases with GV speed, specially the error of the markers positions, as can be seen in Fig. 5. This can be caused by the linearization required by the EKF and the discrete-time formulation. The increase of the GV velocity decreases the predictive capacity of both models, for the EKF constant sampling time T_s.

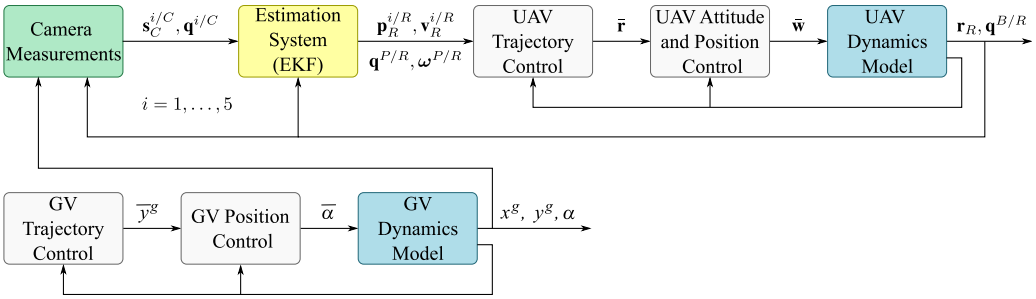

Figure 2. Representation of interaction between the modeled systems.

Table 1. Parameters adopted in simulation.

Parameter	*Value*	**Parameter**	*Value*	**Parameter**	*Value*
m	$1.2\ [kg]$	k_d	3.08×10^{-7}	$\mathbf{F}^g$	$[0\ 0\ g]^\top\ [N]$
$\mathbf{J}$	$diag(0.15, 0.015, 0.03)\ [kg \cdot m^2]$	k_p	1.00	d	$3.5\ [m]$
k_m	1.28×10^{-5}	l_1	$0.25\ [m]$	τ_s	$1.0\ [s]$
τ_m	$0.1\ [s]$	l_2	$0.25\ [m]$	θ_{max}	20º

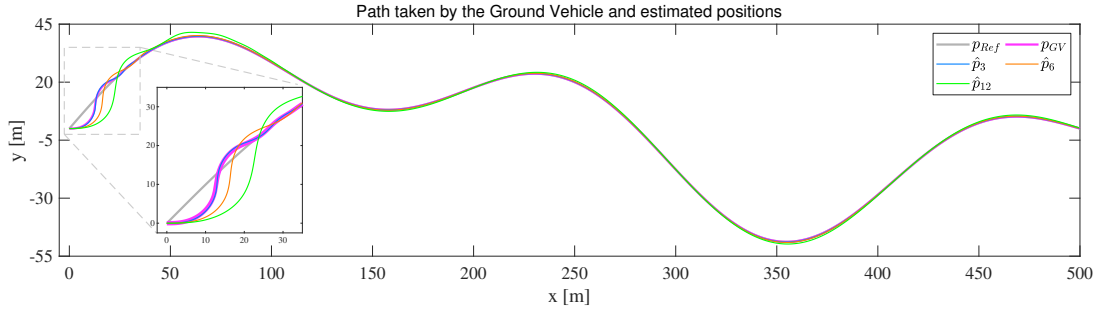

Figure 3. Comparison between the reference path, the path taken by the GV and the estimated value of $\mathcal{S}_P$ path, in the three cases C1 ($\hat{p}_3$), C2($\hat{p}_6$), and C3 ($\hat{p}_{12}$).

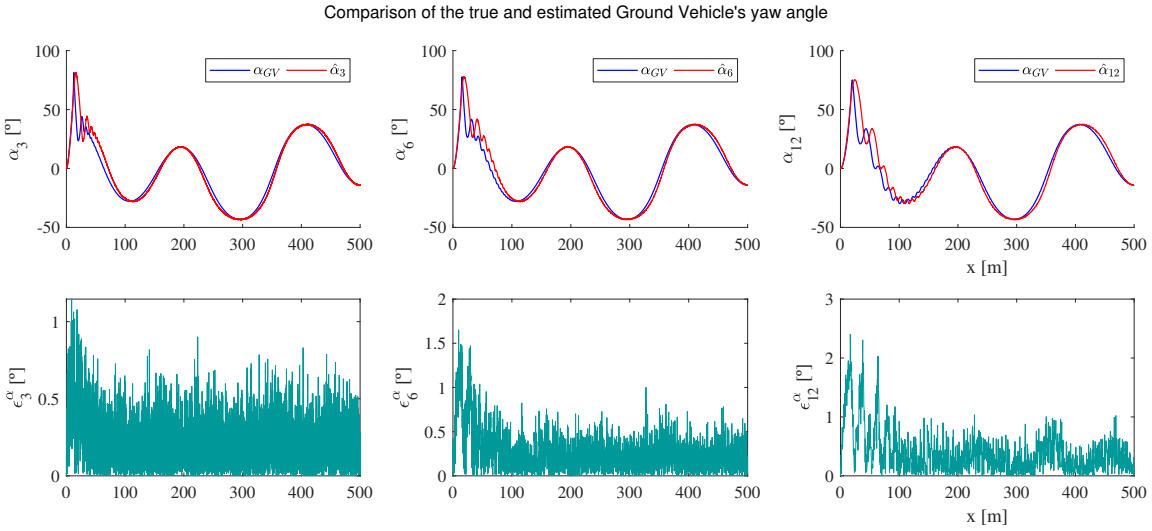

Figure 4. Comparison between the true and estimated angle of orientation of the GV (equivalent to the LP) and the estimation error for the cases C1 ($\hat{\alpha}_3$ and ϵ_3^α), C2 ($\hat{\alpha}_6$ and ϵ_6^α), and C3 ($\hat{\alpha}_{12}$ and ϵ_{12}^α). The quaternion is converted to the Euler angles parameterization, in the sequence 123, see Markley and Crassidis [4, p. 364].

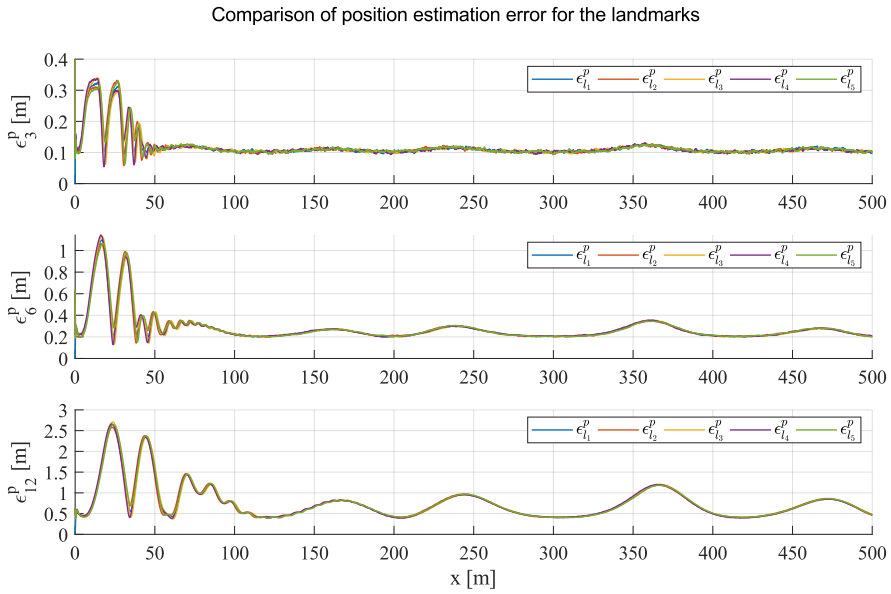

Figure 5. Estimation error (ϵ) for each one of the five markers on the LP ($l_1, \ldots l_5$) for the cases C1, C2, and C3.

5 Conclusions

The simulation results showed that the proposed formulation fulfills the objective of estimating the position and orientation of the landing platform on top of the ground vehicle. The proposed discrete-time Extended Kalman Filter formulation provides an easy implementation for embedded computers and presented a satisfactory result at low speeds, but decreasing its performance as the GV speed increases. The next step is to evaluate this proposition with an experimental setup with alternatives formulations for the filter, in order to better deal with the nonlinearities of the model.

Authorship statement. The authors hereby confirm that they are the sole liable persons responsible for the authorship of this work, and that all material that has been herein included as part of the present paper is either the property (and authorship) of the authors, or has the permission of the owners to be included here.

References

[1] S. Garrido-Jurado, R. Muñoz-Salinas, F. Madrid-Cuevas, and R. Medina-Carnicer. Generation of fiducial marker dictionaries using mixed integer linear programming. *Pattern Recognition*, vol. 51, pp. 481–491, 2016.
[2] F. J. Romero-Ramirez, R. Muñoz-Salinas, and R. Medina-Carnicer. Speeded up detection of squared fiducial markers. *Image and Vision Computing*, vol. 76, pp. 38–47, 2018.
[3] M. Shuster. A survey of attitude representation. *Journal of The Astronautical Sciences*, vol. 41, 1993.
[4] F. L. Markley and J. L. Crassidis. *Fundamentals of Spacecraft Attitude Determination and Control*. Springer New York, New York, NY, 2014.
[5] M. E. Pittelkau. An analysis of the quaternion attitude determination filter. *The Journal of the Astronautical Sciences*, vol. 51, n. 1, pp. 103–120, 2003.
[6] K. Popp and W. Schiehlen. *Ground Vehicle Dynamics*. Springer Berlin Heidelberg, 2010.
[7] P. Polack, F. Altche, d'Andrea B. Novel, and de A. La Fortelle. The kinematic bicycle model: A consistent model for planning feasible trajectories for autonomous vehicles? In *2017 IEEE Intelligent Vehicles Symposium (IV)*. IEEE, 2017.
[8] R. Mahony, R. W. Beard, and V. Kumar. Modeling and control of aerial robots. In *Springer Handbook of Robotics*, pp. 1307–1334. Springer International Publishing, 2016.
[9] H. Fang, N. Tian, Y. Wang, M. Zhou, and M. A. Haile. Nonlinear bayesian estimation: from kalman filtering to a broader horizon. *IEEE/CAA Journal of Automatica Sinica*, 2018.
[10] Y. Bar-Shalom, X. R. Li, and T. Kirubarajan. *Estimation with Applications to Tracking and Navigation: Theory Algorithms and Software*. Wiley-Interscience, 1 edition, 2001.